bjh british journal of haematology

Synergistic intracellular iron chelation combinations: mechanisms and conditions for opimising iron mobilisation

Journal:	*British Journal of Haematology*
Manuscript ID:	BJH-2014-02226
Manuscript Type:	Ordinary Papers
Date Submitted by the Author:	23-Dec-2014
Complete List of Authors:	Vlachodimitropoulou Koumoutsea, Evangelia; UCL, Haematology Garbowski, Maciej; UCL, Haematology Porter, John; UCL, Haematology
Key Words:	CHELATOR, TRANSFUSION, THALASSAEMIA

Synergistic intracellular iron chelation combinations: mechanisms and conditions for opimising iron mobilisation

ABSTRACT (250)

Iron chelators are increasingly combined clinically but the optimal conditions for cellular iron mobilisation and mechanisms of interaction are unclear. Speciation plots for iron(III) binding of paired combinations of the licensed iron chelators desferrioxamine (DFO), deferiprone (DFP) and deferasirox (DFX) suggest conditions under which chelators can combine as 'shuttle' and 'sink' molecules but this approach does not consider their relative access and interaction with cellular iron pools. To address this issue, a sensitive ferrozine based detection system for intracellular iron removal from the human hepatocyte cell line (HUH-7) was developed. Antagonism, synergism or additivity with paired chelator combinations was distinguished using mathematical isobologram analysis over clinically relevant chelator concentrations. All combinations showed synergistic iron mobilisation at 8h with clinically achievable concentrations of sink and shuttle chelators. Greatest synergism was achieved by combining DFP with DFX, where about 60% of mobilised iron was attributable to synergistic interaction. These findings predict that the DFX dose required for a half maximum effect can be reduced by 3.8 fold when DFP at only 1μM is added. Mechanisms for the synergy are suggested by consideration of the iron-chelate speciation plots together with the size, charge and lipid solubilities for each chelator. Hydroxypyridinones with low lipid solubilities but otherwise similar properties to DFP were used to interrogate the mechanistic interactions of chelator pairs. These studies confirm that synergistic cellular iron mobilisation, requires one chelator to have the physicochemical properties to enter cells, chelate intracellular iron and subsequently donate iron to a second 'sink' chelator.

INTRODUCTION

Repeated blood transfusions, such as to patients with thalassaemia major, leads to inexorable accumulation of body iron unless chelation therapy is given. Iron accumulates first in the macrophage system, subsequently into hepatocytes, finally escaping extrahepatically into the myocardium and endocrine system risking damage to these tissues. Despite the clinical availability of three iron chelators, some patients fail to adequately respond to chelator monotherapy. The proportion of body iron available for chelation at any moment in time is finite, as direct chelation of storage iron is slow, and derived from two key iron 'pools' namely red cell catabolism and turnover of intrahepatic iron stores. Consequently chelation monotherapy tends to be 'inefficient' : for example with deferiprone monotherapy only about 5 % of the chelator binds iron before being eliminated from the body (Yesim Aydinok, *et al* 2013).

The iron chelators, desferrioxamine (DFO), deferiprone (DFP) and deferasirox (DFX) have been licensed for clinical use as monotherapies. Combination therapies, may theoretically improve chelation efficiency by increasing the rate of access to intracellular iron pools (Yesim Aydinok, *et al* 2013) or to plasma non-transferrin bound iron (NTBI) (Evans, *et al* 2010). The most extensively studied combination clinically is the parenteral chelator DFO with the oral chelator DFP (Tanner, *et al* 2007). This combination has often been given sequentially (Tanner, *et al* 2007) (Aydinok, *et al* 2007), where one follows the other but some regimes contain overlap or simultaneous co-administration (Porter, *et al* 2013). Accelerated decrements in serum ferritin (SF), liver iron (LIC) (Aydinok, *et al* 2007) and heart iron (Tanner, *et al* 2007) have been reported relative to monotherapy. Combination of the orally active DFX with DFO has also had some clinical evaluation (Lal, *et al* 2013) and is the subject of further prospective trials (Aydinok, Hyeprion Abstract ASH 2014). The combination of two orally chelators, DFP with DFX, would be more appealing to patients than therapies involving parenterally administered DFO but clinical experience is limited(Elalfy, *et al* 2013).

It remains unclear to what extent any improved chelation with such combinations is a consequence of true drug interaction or simply due to increased overall exposure to chelation. In principle, when two chelators are combined they may act additively, synergistically or have no improved effect compared with monotherapy. Additivity refers to the predicted effect achieved by a drug combination, based on individual drug potencies, whilst synergy refers to

the exaggerated effect. Chelation synergism may occur in conditions allowing 'iron shuttling', whereby a chelator with rapid access to iron pools, donates iron to a chelator that has slower kinetic access but can act as a 'sink', or stable acceptor for iron initially chelated by the shuttle molecule (Evans, *et al* 2010). This mechanisms has previously been demonstrated in plasma with non-transferrin bound iron (NTBI) where low concentrations of DFP act as the 'shuttle' by gaining more rapid access to some NTBI species than DFO, and subsequently donating iron to the DFO 'sink' (Evans, *et al* 2010). The rates at which individual chelators gain access to and mobilise intracellular iron is determined by size, charge and lipid solubility of the chelators in question both *in vitro* (Porter, *et al* 1988) (Hoyes and Porter 1993) (Porter, *et al* 2005) and *in vivo* (Porter, *et al* 1990). However, the rates and optimal conditions under which paired combinations of the three licensed chelators interact with and mobilise intracellular iron pools have not been compared directly. Here we have systematically investigated the time course and concentration dependence for paired combinations of these chelatprs. Total cellular iron has been measured using a sensitive ferrozine assay and the rates of intracellular iron mobilisation examined in human hepatocyte-like cells (HuH7) (Nakabayashi, *et al* 1982). Isobologram analysis (Tallarida 2006 {Grabovsky, 2004 #23612) has been used to distinguish between synergistic, additive or a subadditive responses. Further insights into the mechanisms of enhanced chelation have been sought by using highly hydrophilic hydroxypyridinone iron chelators that do not access intracellular iron.

MATERIALS AND METHODS (500)

***The cellular model*:** HuH-7 cells were plated at 200,000 cells/well with RPMI 1640 supplemented with 10% FBS, 0.02% penicillin and 0.5% gentamycin. 24 hours cell attachment was allowed. Supernatant (10% FBS) was changed twice at 10 hour intervals. A threefold increase in intracellular iron concentration was achieved (from 12 to 36nmol/mg protein) , more efficiently than with ferric ammonium citrate (FAC) (**data not shown**). The cells were sequentially washed with PBS, 90μM DFO/PBS for 1 minute then PBS. After incubation with test chelators, further washes with PBS (x3), 90μM DFO/PBS then PBS were performed.

Cell damage and viability: have a critical influence on cellular iron release (Porter*, et al* 1988) and > 98% was achieved in all reported experiments. Viability staining by dye included both 0.4% Trypan blue and Acridine Orange (AO)/Propidium Iodide (PI). Microscope images were captured.

Iron determination by the ferrozine assay: Cells were lysed overnight with 200μL of 200mM NaOH. Ferosine assay (on 190μL aliquots) were as per Riemer et al[13]. 120μL of iron-detection reagent (6.5mM ferozine, 6.5mM neocuproine, 2.5M ammonium acetate, and 1M ascorbic acid dissolved in iron free HPLC grade water) were added for 30 minutes. Absorbance was recorded at 562nm and lysate iron content calculated by standard curve intrapolation against atomic absorption iron standards. Intracellular iron was normalized against protein content.

Protein Assay: was determined as per the Coomassie (Bradford) protocol: 250μL of Bradford reagent were added to 5μL of cell lysate in duplicates and absorbance recorded at 595nm against a standard curve generated from BSA.

Chelators studied: are shown in **Table 1** together with their physicochemical properties. The structures of DFO, DFP and DFX have been previously published (Porter and Hershko 2012) while the hydroxypyridinones CP40 and CP46 are closely related to the 1,2,dimethyl,3-hydroxypyridinone DFP but possess $(CH_2)_2OH$ or $CH_2CH_2CH_2NH_3^+Cl^-$ substitutions respectively in the nitrogen postion of the pyridinone ring, rendering them highly hydrophilic (**Table 1**) (Dobbin*, et al* 1993). DFO meyslate was purchased from Novartis; DFP, DFX, CP40 and CP46 were synthesised in the laboratory of Hider, Kings College London.

Speciation Plots: Speciation plots in **Figure 1** show the molar fraction of iron bound to chelators at physiological pH at equilibrium, calculated using HYSS as previously described in which the concentrations of iron and DFO are constant at 10mM and the concentration of DFP was varied. The stability constants were from published data (Motekaitis and Martell 1991).

Non-linear regression analysis of iron mobilization: Statistical analysis of the curves in **Figures 3 A, B and C** used prism 5 software. Curves were plotted using non-linear regression of log (inhibitor) vs. response modeled by the formula 'Y=Bottom + (Top-Bottom)/(1+10^((LogIC$_{50}$-X)*HillSlope))' with shared 'Top' and 'Bottom' between conditions (not shown). The extra sum of squares F-test was used to compare the IC$_{50}$ values for each dose of the scaled chelator combination. The test was significant ($p < 0.0001$) in all three cases, indicating significant difference in the IC$_{50}$ values at increasing chelator concentrations. Akaike's information criterion was used to for relative goodness of fit and was > 99 % for the constructed fits.

RESULTS

Speciation Chelator Plots and their relevance to synergistic chelator combinations

Speciation plots for paired combinations predict the binding of iron(III) by each chelator at equilibrium under defined conditions. These provide indications of which chelator has the potential to act as a shuttle or sink over the concentration ranges shown. These proportions are based on the known stability constants and chelation denticity (ratio of binding for chelator:iron). Plots are for steady state solutions and do not account for the kinetics of this interaction.

The molar fraction of 10μM iron(III) bound to 10μM DFO in the presence of increasing concentrations of DFX is presented in **Figure 1A**. At 10μM DFO, equilibrium favors the formation of iron complexes of DFO until those of DFX exceed about 15μM. This predicts that DFX will act as a shuttle for iron(III) onto DFO at concentrations < 20μM but at higher concentrations may compete with DFO as a sink for iron(III). Thus at clinically achieved trough concentrations (about 20μM) (Galanello, *et al* 2006) (Piga, *et al* 2006, Waldmeier, *et al* 2010), using standard daily DFX dosing, about half of iron(III) is predicted to be bound to DFO and half to DFX at neutral pH such as plasma. At peak clinical DFX concentrations (about 60μM), equilibrium will favor the predominance of DFX iron complexes over those of

DFO. Thus at trough DFX concentrations iron(III) will potentially be donated to DFO, whereas this is less likely at peak DFX concentrations. As this prediction is for a cell free system and does not predict the rates at which equilibrium is obtained, subsequent studies in the cell based system were performed.

The influences of varying the concentrations of DFP and DFX on the proportion of iron(III) bound to mixtures of each chelator is presented in **Figures 1B** and **C**. **Figure 1B** shows the molar fraction bound to 30μM DFP at increasing concentrations of DFX, indicating for example at 10μM DFX about half of the iron(III) is bound to each chelator, but when DFX exceeds 10μM the iron complex of DFX increasingly predominates. Thus at clinically relevant trough and peak concentrations of DFX about 40% and >98% respectively of iron(III) is predicted to be bound to DFX. **Figure 1C** shows the speciation of iron-chelate complexes at constant concentrations of 20μM DFX with increasing concentrations of DFP. These confirm **Figure 1B** but also allow examination of higher DFP concentrations. Peak clinical DFP concentrations of 100μM have been reported (Limenta*, et al* 2011) (Morales*, et al* 2009) (Jirasomprasert*, et al* 2009) and under these concentrations and at trough concentrations of DFX about 60% of iron(III) is predicted to be bound to DFP. This analysis suggests a 'push–pull' effect for iron free binding over the range of clinically achieved concentrations, providing conditions for both shuttle and sink effects to occur.

The speciation plot for the molar fraction bound to DFO at increasingly concentrations of DFP is presented in **Figure 1D** as published by our group (Evans*, et al* 2010). At clinically relevant 10μM iron (III) and 10μM DFO, DFO iron binding predominates until the concentration of DFP exceeds 1mM (not achieved clinically). At clinically relevant peak DFP concentrations of 100μM, about 5% of iron(III) will be bound by DFP at equilibrium. This implies that considerably higher concentrations of DFP than of DFX are required to compete with DFO for iron(III). Thus combinations DFO differ between DFX or DFP: while the DFO iron(III) complexes will predominate at all clinically achievable DFP concentrations, the proportion bound to DFO when combined with DFX depends on whether DFX is at peak or trough levels.

Monotherapy iron mobilisation time course with DFO, DFP and DFX

Intracellular iron removal was investigated over time in the presence of DFP, DFX or DFO at 10μM (ibe) and 30μM ibes (**Figure 2A, B)**. Whereas this decreased with DFX and DFP as early as 1h, there was no decrease until after 4h with DFO (**Figures 2A,B,C**). Following 8h, the iron removal was similar for all three chelators.

Comparative cellular iron with mobilisation with monotherapy and combinations

Responses at 8h are plotted in **Figures 3 A, B**, **and C** as a function of ibe vs iron/protein, where the concentration of a second chelator (or no chelator) are constant. DFO monotherapy showed concentration dependent cellular iron removal at 8h (**Figure 3 A, B**) in contrast to findings at 4h above. Iron mobilization with DFX (**Figure 3 A, C**) or DFP (**Figures 3 B, C**) showed concentration dependence which was greater than at 4h. When a second chelator was added, there was a significant additional decrease in intracellular iron across the range of concentrations of the first chelator. Using non-linear regression, small increments of one chelator have statistically and biologically significant chelation effects. **Figure 3 E** shows that at 4h when DFO alone has no iron mobilising effects, significant additional iron removal is seen when combined with DFP. Thus DFO can act as an extracellular sink at short time intervals when cell uptake and direct access to intracellular iron with DFO is limited.

Differentiation of synergy vs additivity of chelator combinations using isobolograms

The isobolgram is a mathematical model to distinguish between synergistic, additive or sub-additive response of drug combinations (Tallarida 2006) where rectangular coordinates of dose combinations (a,b) that produce the same chosen effect level are shown ; often 50% of maximum response. In its classical form, this plot is constructed as a straight line of additivity connecting the x and y intercepts that represent the individually effective doses, for example the IC_{50} values of each chelator monotherapy. This line is the reference for distinguishing additive from synergistic or sub-additive interactions. **(Figure 4A)**.

Figures 4 **B, C** and **D** present the isobolograms for combinations of the three commercially used chelators for a 50% chelation effect (half maximal of the chelatable iron pool) following 8h of chelator treatment: the axis intercepts represent the IC_{50} for each chelator used in isolation (ie the potency; eg 12.5μM ibe for DFX). The straight line connecting these intercept points is the line of potential additivity and represents the locus of all such dose pairs, which based on their known potencies, should give the same chelation effect. In all

three cases, combined chelators produce a curved response below the line of additivity, indicating synergism. Lines were also constructed for 20 and 30% effects (not shown) and used for EC20, 30 and 50 data presented in **Table 2**.

Indexes of synergy with the three combinations

Synergy Index α

This index is a representation of how much of the obtained effect exceeds that expected by additivity. The synergy index α, is equivalent to $(1 - 1/A)\ X\ 100$ where A = difference of area under the line and area under the curve. This index has been previously used to examine synergy (Tallarida 2006), and was derived using data generated from 'Prism 5'. It was noted that when DFX and DFO are combined, 37% of the chelation effect is due to synergy compared with 47.4% in the case of the DFP-DFO combination. The synergistic effect is even greater, at 51.5% in the case of the two oral chelators DFP and DFX (**Table 2**).

Combination index

The software calcusyn 2.1 (purchased from www.biosoft.com was used to provide a combination index 'CI' for each chelator pair. A CI < 1 indicates synergy whilst a CI > 1 indicates antagonism. Thus the lower the CI value <1, the greater the synergy. The combination with the lowest CI and hence greatest synergy is again DFP plus DFX. It was once again indicated that the most synergistic pair was the combination of the two oral chelators DFP and DFX with a CI of 0.38 (**Table 2**).

Dose reduction index

In order to demonstrate how combined chelation impacts on the chelator dose required to achieve a given effect, a dose reduction index (DRI) was calculated from data in 3 using the program calcusyn 2.1 (**Table 3).** The DRI is an estimate of the ratio of the dose required for a given effect, before and after the addition of a second chelator. Thus, for example, when DFP is added to DFX, the dose of DFX can be reduced by 3.8 fold when only 1μM ibe DFP is achieved in the blood. This implies that the standard dose of 25mg/kg/day of DFX can be reduced to about 5mg/kg/day if DFP is added to achieve the concentration shown in column 3 of **Table 3**.

Insights into synergistic mechanisms using the hydroxypyridinones CP40 and CP46 as probes

The highly hydrophilic bidentate hydrypyridinine chelators CP40 and CP46 were used to probe the mechanism of combined chelator. No iron is mobilised from hepatocytes or from iron overloaded mice due to their low lipid solubility and inability to penetrate the cell membrane (Porter, *et al* 1988) (Porter, *et al* 1990) compared to the closely related DFP. In **Figure 2D and Figure 3D**, in contrast to DFP, DFX or DFO, CP40 monotherapy does not enhance cellular iron removal, consistent with observations in primary hepatocytes (Porter, *et al* 1990). This also validates the integrity of the cell membrane in the cell culture model, because any cells with damaged or leaky cell membranes would allow intracellular iron to be chelated by the hydrophilic chelators. This also supports DFO, DFX and DFP as acting exclusively and directly on intracellular pools in **Figures 2 A, B, C**.

When CP40 100μM was combined with DFO, no additional increased iron removal was observed over at 8h (**Figure 3D**) but when CP40 was combined with DFP or DFX, a small increase in cellular iron removal was seen. This provides mechanistic insight into how chelator combinations interact: firstly it supports DFO as an acceptor or 'sink' for iron (III) in combined therapy. DFO can only act as an acceptor for iron(III) due to its hexadentate structure and high pM (**Table 1**, **Figure 1**). Thus because CP40 has very little access to intracellular iron when used alone, it cannot act as an intracellular iron shuttle onto extracellular DFO. When CP40 combined with DFP however, the additional iron mobilisation observed (**Figure 4D**) is consistent with CP40 increasing the magnitude of the extracellular sink for iron(III). Likewise the small increase in cellular iron mobilisation observed when CP40 was combined with DFX (**Figure 3D**) is likely due to an increase in the extracellular 'sink' total concentration. This is supported by speciation plot analysis of DFP (which has similar iron binding properties to CP40): at 30μM DFP and 30μM DFX, about 20% of the iron(III) binds to DFP (and hence CP40) rather than DFX. Thus the small increase in iron mobilisation when CP40 is added to DFX is consistent with an increase in the concentration of extracellular 'sink'.

DISCUSSION

Findings with monotherapies provide a framework for understanding the potential effects for combined chelator pairs. All three clinically available chelators are effective as monotherapy in this cell system and at clinically relevant concentrations. However, little cellular iron removal occurs with DFO before 4 hours, consistent with previous reports of slower access to intracellular iron than with DFP or other hydroxypyridinones (Cooper, *et al* 1996, Hoyes

and Porter 1993). This is attributable to the relatively low lipid solubility of DFO and its larger size than DFP (Porter, *et al* 2005). Furthermore, the iron complex of DFO is slow to egress from cells (Cooper, *et al* 1996, Hoyes and Porter 1993) due to its positive charge and low lipid solubility (Cooper, 1996 #1610}(Porter, *et al* 2005). As with previous studies, the highly hydrophilic chelators CP40 and CP46, which otherwise have similar iron binding properties to DFP, induced no iron release as monotherapies (Porter, *et al* 1988) (Dobbin, *et al* 1993). This has been attributed to the necessity of chelators to access intracellular iron directly by transiting the cell membrane in both the iron free and complexed states.

For paired combinations of the licensed chelators, this study is to our knowledge is the first attempt to formally distinguish between synergy and additivity: concentrations were chosen to be clinically relevant. Our findings indicate synergistic interaction with all three chelator pairs. This conclusion is based firstly on the shapes of isobol plots, using established general methods for comparing drug interactions (Tallarida 2006). Synergy is also supported by the results with the computed combination index and the synergy index derived from the isobolograms. In all three analyses, the combination of DFX and DFP shows greater activity at 8h than the other combinations. Our findings show that synergistic interaction depends on their iron binding affinities, their relative concentrations and their ability to access intracellular iron pools directly.

The likely mechanism of synergy with combined DFO and DFP is the rapid access of DFP to intracellular iron with subsequent donation of chelated iron to DFO, the latter providing a predominantly extracellular sink for iron chelated by DFP. This mechanism has been previously demonstrated for NTBI in a cell free system where DFP can access some NTBI species more rapidly than DFO (Evans, *et al* 2010). DFP, by virtue of its low molecular weight, neutral charge and lack of extreme hydrophilicity can enter cells and exit rapidly as the iron complex. Additionally it has more rapid access to iron pools within (Hoyes and Porter 1993) (Porter, *et al* 2005) (Glickstein, *et al* 2005) (Glickstein, *et al* 2006) and outside cells (Evans, *et al* 2010) more rapidly than DFO and is thus an ideal molecule for shuttling purposes. Inspection of speciation plots shows that at equilibrium, iron is ultimately destined to binding to DFO when paired with DFP.

The synergism between DFX and DFO depends firstly on the faster access of DFX than DFO to cellular iron and subsequently the faster egress of the iron-chelate complex of DFX. This DFX chelated cellular iron then needs to be donated to DFO extracellularly. Faster access of

DFX to cellular iron is shown in the monotherapy experiments and is consistent with the known higher lipid solubility and lower molecular weight of DFX compared with DFO. Subsequent donation of DFX chelated iron to DFO is consistent with the speciation plots (**Figure 1**) and iron binding stoichiometry of these two chelators : because of the hexadentate iron binding of DFO, the iron complexes are highly stable at neutral pH and will not act as an iron 'shuttle'. However because of its tridentate 2:1 stoichiometry, the iron complex of DFX is less thermodynamically stable than iron complexes of DFO and hence of some or all of the iron chelated by DFX (depending on relative concentrations) is donated onto DFO. This provides the circumstances for shuttling and hence for synergy with this combination. Nevertheless the speciation plots suggest that within cells DFX may compete to some extent for iron binding with DFO when DFX concentrations exceed about 10μM. However the main synergistic mechanism is for DFO is to provide an extracellular sink for some or all of the iron rapidly chelated by DFX, subsequently freeing DFX to shuttle back for further rounds of intracellular chelation.

Synergism of DFP combined with DFX is more complex because both chelators have rapid access to intracellular iron and both have the potential to act as either shuttles or sinks for iron(III), depending on their relative concentrations. Consideration of speciation plots shows that over typical ranges seen with DFX clinically (20-60μM), that DFX will act more as a 'sink' for iron chelated by DFP except at peak concentrations of DFP (100μM) where this molecule will compete with DFX. The speciation analysis does not take into account the rates of access or the compartmentalization of chelatable cellular iron however. The monotherapy data (**Figure 2**) showed that DFX gains sufficient intracellular access to mobilise iron with similar kinetics to DFP. However, while both chelators have rapid access to intercellular iron pools (Hoyes and Porter 1993) (Porter, *et al* 2005) (Glickstein, *et al* 2005) (Glickstein, *et al* 2006), it is also possible that DFP can access additional intracellular pools that are only slowly available to DFX (Glickstein, *et al* 2005) (Glickstein, *et al* 2006).

Combinations of chelators with CP40 or CP46 provide further mechanistic insight into the actions of DFP in combination therapy, particularly when DFP is combined with DFX. Even though CP40 and CP46 cannot gain direct access to intracellular iron (**Figures 2D**), when combined with a chelator that can shuttle iron (such as DFX or DFP but not DFO) they increase cellular iron release (**Figure 3D**). Speciation plots for CP40 or CP46 (not shown) are very similar to DFP and suggest that CP40 or CP46 have the potential to act as an extracellular sink for iron chelated by DFX. For example at 20μM DFX, even at low concentrations of a hydroxypyridinone (10μM) about 10% of iron(III) be bound to a hydroxypyridinone (**Figures 1 B and C**). Furthermore at 100μM about 40% of the iron will

bind to the hydroxypyridinone thereby effectively increasing the 'sink' chelator concentration. This extracellular 'sink' effect for CP40 or CP46 will also be seen with DFP when combined with DFX. Hence when combined with DFX, DFP has the potential to act both as a shuttle and a sink for iron(III) suggesting a mechanism by which this combination is particularly effective.

In conclusion, our findings indicate that all three clinically available chelators can act in synergy when paired with another chelator but that the combination of DFP with DFX is likely to be the most potent. When DFP is added to DFX, the dose DFX dose can be reduced by 3.8 fold when only 1μM ibe DFP is achieved in the blood. This implies that the standard dose of 25mg/kg/day of DFX could be reduced to about 5mg/kg/day when consitent plasma concentrations of only 1μM ibe are achieved. Further well-controlled clinical trials that also examine the safety of this combination are warranted. Additional studies on other cell types such as cardiomyocytes would clarify if the mechanisms observed here apply to other cell types where transfusional iron can accumulate.

Acknowledgements

We would like to thank the Onassis Foundation, Athens, Greece for the support of this work in the form of a Scholarship for Dr Vlachodimitropoulou Koumoutsea.

- Dr Vlachodimitropoulou Koumoutsea performed the research
- Dr Vlachodimitropoulou Koumoutsea and Prof Porter designed the research study
- Dr Vlachodimitropoulou Koumoutsea, Dr Maciej Garbowski and Prof Porter contributed essential reagents or tools
- Dr Vlachodimitropoulou Koumoutsea analysed the data
- Dr Vlachodimitropoulou Koumoutsea and Prof Porter wrote the paper.

LEGENDS

TABLE 1 The physicochemical properties of the studied chelators are shown, based on published data on DFO (Porter, *et al* 2005), DFP (Dobbin, *et al* 1993) and DFX (Nick, *et al* 2002, Porter 2006) and CP40 (Porter, *et al* 1988) and CP46 (Dobbin, *et al* 1993). The lipid solubilities of the free ligand and their major iron(III) complexes are shown as the ratio of the chelator in N-octanol (Dobbin, *et al* 1993) : water (pH 7.4). Chelators with the exception of DFX, have a Kpart <1 and are therefore hyrdophilic. DFP is the least hydrophilic of the hydroxypyridinones studied and is also neutrally charged: both properties favouring rapid access of the free ligand and its iron complex from cells (Porter, *et al* 1988). The positive charge of DFO facilitates cellular uptake of the free ligand but the positive charge of the iron complex retards its egress from cells (Porter, *et al* 2005). For DFX the high lipid solubility will encourage cell uptake but the negative charge of the free ligand of DFX may retard this (Porter, *et al* 2005) while the negative (3-) charge of the iron complex will encourage egress of the iron complex from cells. CP40 and CP46 are predicted to have slow cellular uptake by virtue of their very low lipid solubility(Porter, *et al* 1988) (Dobbin, *et al* 1993). The relative stabilities of iron(III) binding can be represented by the pM values, where the pM of a given chelator for a metal (M) and iron(III) is the negative log of the uncoordinated metal concentration under defined conditions(Martell 1981). When pairs of chelators are combined in solution, iron (III) will bind preferentially to the chelator with the higher pM value. This is highest for DFO (Ihnat, *et al* 2002) and lowest for the hydroxypyridnones including DFP (Motekaitis and Martell 1991) with DFX having an intermediate value (Nick, *et al* 2002). The consequences of these differences are reflected in the relative proportions of iron(III) bound to pairs at equilibrium as shown in speciation plots in Figure 1.

TABLE 2 shows the combination index (CI) and synergy index (α) for each combination of chelators, derived from data in Figure 3 : a low combination index indicates a greater synergistic effect. The ED (median effective dose of combined chelators at a 1:1 ratio in ibe) is shown for a 20%, 30% and 50 % effect (ie % of total cellular iron removed). The lowest ED at each effect level (ie most synergistic) is for the combination of DFX + DFP. The linear correlation coefficient of the median effect plot, R, is also shown and indicates a high level of cofrormity for the model used. The synergy index 'α' for combinations of chelators is also shown (column six) as described in methods. A synergistic effect is present for all combinations but is greatest, at 51.5%, for combinations of DFP with DFX.

TABLE 3 shows the dose reduction index (DRI) for 50% cellular iron removal for three chelator combinations, where the DRI is an estimate from data in figure 3 of the ratio of the dose require for a given effect before and after the addition of a second chelator. Thus the higher the DRI, the greater the effect of the combination (column 2). Examples of the shuttle (column 3) and sink chelator concentrations (column 4) achieving the DRI are also shown. Thus for example with the DFX-DFP combination, only 0.9μM ibe of DFP decreases the concentration of DFX required to achieve a given effect by 3.8 times compared to DFX monotherapy.

TABLE 4 demonstrates the impact of incresing doses of DFP (column 1) on the DFX dose required for a 50% effect (? 50%decrease in cellular iron?) . It can be seen in colum two that as the DFP concentration increases, the DFX concentration required for a 50% effect decreases. Column three shows the dose reduction index (DRI), which is the difference between the monotherapy mose of DFX required for a 50% effect and DFX dose required when combined with DFP at the concentrations shown in column 1. In column four, the estimated impact of the DRI on the dose of DFX required for a 50% effect is shown as the reduction of DFX dose that may be given to achieve the same effect as when used as monotherapy. Thus for example a plasma concentration of DFP as low 5μM is predicted to decrease the oral dose of DFX required by 10.6mg/kg/day.

FIGURE 1. The speciation plots show the steady state molar fraction of chelator bound iron (III) at increasing concentrations of a second chelator under defined conditions, namely 10μM iron (III) and at pH 7.4**.** The speciation plot was calculated using HYSS (Alderigh*, et al* 1999) and the stability constants used for the calculations are from published data referenced in Table 1. (**A**) shows the molar fraction of iron(III) bound to 10μM DFO with increasing concentrations of DFX. **(B)** shows the molar fractions bound to DFX or DFP, at a constant 30μM DFP, with increasing concentrations of DFX : whereas at 10μM DFX about half of the iron (III) is bound to each chelator, at higher DFX concentrations the complexes of DFX predominate. (**C**) shows the molar fractions at 20μM DFX, and with increasing concentrations of DFP. Equilibrium favours DFX iron complexes until [DFP] exceeds 100μM. **(D)** shows the molar fraction of iron (III) bound to 10μM DFO at increasingly concentrations of DFP which has been previously published by our group (Evans*, et al* 2010) : iron binding to DFO predominates until the concentration of DFP exceeds 1mM. Thus a considerably higher concentration of DFP is required to compete for iron binding with DFO than with DFX. Also however 100μM DFP will compete for iron binding with DFX but not DFO.

FIGURE 2. Cellular iron retention is shown as a function of time of exposure to different single chelators at 10μM iron binding equivalents ibe (A) or 30μM ibe (B) or as a function of varying chelator concentrations at 4 hours (C) and 8 hours (D). Following iron loading as described in Figure 2, the cells were rinsed four times including one wash containing DFO at 30μM ibe and 3 PBS washes, and subsequently exposed to DFP, DFX or DFO. At the end of the incubation period, chelator supernatants were removed and the cells further washed three times as above and lysed with 200mM NaOH. Intracellular iron concentration was then determined using the ferrozine assay and expressed as a function of total cellular protein.

Need to decide whether to use h or hours.

FIGURE 3 Cellular iron retention is shown after 8h exposure to single chelators or to chelator combinations **(A)** DFO or DFX monotherapy at varying concentrations or DFO + DFX at varying concentrations of DFX. **(B)** DFO or DFP monotherapy at varying concentrations or DFO + DFP at varying concentrations of DFP. **(C)** DFP or DFX monotherapy at varying concentrations or DFP + DFX at varying concentrations of DFX. When the chelators were used in combination, there was a significantly greater reduction in intracellular Fe(II) compared to chelator monotherapy. Reduction in cellular iron was noted with as little as 1μM ibe and was significantly greater for combinations of DFP+ DFX, DFO + DFP and DFP+ DFX than for monotherapies. ($p<0.001$ for Log IC50 values of monotherapy compared with combination therapies). **(D)** Cellular iron retention is shown with monotherapies (10μM) or combination therapies of the chelators. It can be seen that CP40 (100μM) has no effect on cellular iron removal and no additional effect when added to DFO. A small additional effect is seen when CP40 added to DFX or DFP at 1μM ibe. **(E)** Cellular iron mobilisations at 4h is shown with DFO or DFP monotherapy and with combined DFO + DFP. DFO monotherapy does not mobilise cellular iron at 4h, but when combined with 10μM DFP ibe, there is a chelation effect significantly greater than either DFO and DFP monotherapy. This further supports the role of DFO as a sink molecule, clearly demonstrated at the 4 hour time point where the chelation effect of DFO in isolation is limited by is low lipid solubility and positive charge affecting chelate eggress.

FIGURE 4 Shows isobologram plots for: (A) an idealised model and for combinations of DFO+DFX (B), DFP+DFX (C), and DFO + DFP (D) The group of isobolograms have been constructed for the 50% of maximal chelation effect on cellular iron release following 8 hours of chelator treatment; the axis intercepts represent the IC50 for each chelator compound used in isolation. The straight line connecting these intercept points is the line of additivity, and

represents the locus of all dose pairs, which based on their potencies should give the same chelation effect. The actual noted effect of tested dose pairs have been linked to produce a curve which in all three combinations tested, is found below the line of additivity indicating a super-additive, namely a synergistic effect.

REFERENCES

Alderigh, L., Gans, P., Ienco, A., Peters, D., Sabatini, A. & Vacca, A. (1999) Hyperquad simulation and speciation (hyss): a utility program for the investigation of equilibria involving soluble and partially soluble species. . *Coord Chem Rev,* **184,** 311–318.

Aydinok, Y., Ulger, Z., Nart, D., Terzi, A., Cetiner, N., Ellis, G., Zimmermann, A. & Manz, C. (2007) A randomized controlled 1-year study of daily deferiprone plus twice weekly desferrioxamine compared with daily deferiprone monotherapy in patients with thalassemia major. *Haematologica,* **92,** 1599-1606.

Cooper, C.E., Lynagh, G.R., Hoyes, K.P., Hider, R.C., Cammack, R. & Porter, J.B. (1996) The relationship of intracellular iron chelation to the inhibition and regeneration of human ribonucleotide reductase. *The Journal of biological chemistry,* **271,** 20291-20299.

Dobbin, P.S., Hider, R.C., Hall, A.D., Taylor, P.D., Sarpong, P., Porter, J.B., Xiao, G. & van der Helm, D. (1993) Synthesis, physicochemical properties, and biological evaluation of N- substituted 2-alkyl-3-hydroxy-4(1H)-pyridinones: orally active iron chelators with clinical potential. *J Med Chem,* **36,** 2448-2458.

Elalfy, M., Wali, Y., Tony, S., A, S. & Adly , A. (2013) Comparison Of Two Combination Iron Chelation Regimens, Deferiprone and Deferasirox Versus Deferiprone and Deferoxamine, In Pediatric Patients With β-Thalassemia Major. *Blood,* **22,** Abstract 559.

Evans, P., Kayyali, R., Hider, R.C., Eccleston, J. & Porter, J.B. (2010) Mechanisms for the shuttling of plasma non-transferrin-bound iron (NTBI) onto deferoxamine by deferiprone. *Translational research : the journal of laboratory and clinical medicine,* **156,** 55-67.

Galanello, R., Piga, A., Forni, G.L., Bertrand, Y., Foschini, M.L., Bordone, E., Leoni, G., Lavagetto, A., Zappu, A., Longo, F., Maseruka, H., Hewson, N., Sechaud, R., Belleli, R. & Alberti, D. (2006) Phase II clinical evaluation of deferasirox, a once-daily oral chelating agent, in pediatric patients with beta-thalassemia major. *Haematologica,* **91,** 1343-1351.

Glickstein, H., El, R.B., Link, G., Breuer, W., Konijn, A.M., Hershko, C., Nick, H. & Cabantchik, Z.I. (2006) Action of chelators in iron-loaded cardiac cells: Accessibility to intracellular labile iron and functional consequences. *Blood,* **108,** 3195-3203.

Glickstein, H., El, R.B., Shvartsman, M. & Cabantchik, Z.I. (2005) Intracellular labile iron pools as direct targets of iron chelators: a fluorescence study of chelator action in living cells. *Blood,* **106,** 3242-3250.

Hoyes, K.P. & Porter, J.B. (1993) Subcellular distribution of desferrioxamine and hydroxypyridin-4-one chelators in K562 cells affects chelation of intracellular iron pools. *British journal of haematology,* **85,** 393-400.

Ihnat, P., Vennerstrom, J. & Robinson, D. (2002) Solution equilibria of deferoxamine amides. . *Journal of pharmaceutical sciences,* **91**.

Jirasomprasert, T., Morales, N.P., Limenta, L.M., Sirijaroonwong, S., Yamanont, P., Wilairat, P., Fucharoen, S. & Chantharaksri, U. (2009) Pharmaco/ferrokinetic-related pro-oxidant activity of deferiprone in beta-thalassemia. *Free radical research,* **43,** 485-491.

Lal, A., Porter, J., Sweeters, N., Ng, V., Evans, P., Neumayr, L., Kurio, G., Harmatz, P. & Vichinsky, E. (2013) Combined chelation therapy with deferasirox and deferoxamine in thalassemia. *Bld cells, molecules & diseases,* **50,** 99-104.

Limenta, L.M., Jirasomprasert, T., Jittangprasert, P., Wilairat, P., Yamanont, P., Chantharaksri, U., Fucharoen, S. & Morales, N.P. (2011) Pharmacokinetics of deferiprone in patients with beta-thalassaemia: impact of splenectomy and iron status. *Clinical pharmacokinetics,* **50,** 41-50.

Martell, A. (1981) *The design and synthesis of chelating agents.* Elsevier North Holland Inc.

Morales, N.P., Yamanont, P., Jirasomprasert, T., Wilairat, P., Chantharaksri, U., Chuncharunee, S. & Fucharoen, S. (2009) Bioequivalence study of a film-coated tablet of deferiprone in healthy Thai volunteers. *International journal of clinical pharmacology and therapeutics,* **47,** 358-364.

Motekaitis, R. & Martell, A. (1991) Stabilities of the iron(III) chelates of 1,2-dimethyl-3-hydroxy-4-pyridinone and related ligands. . *Inorganica Chimica Acta* **183,** 71-80.

Nakabayashi, H., Taketa, K., Miyano, K., Yamane, T. & Sato, J. (1982) Growth of human hepatoma cells lines with differentiated functions in chemically defined medium. *Cancer research,* **42,** 3858-3863.

Nick, H., Wong, A., Acklin, P., Faller, B., Jin, Y., Lattmann, R., Sergejew, T., Hauffe, S., Thomas, H. & Schnebli, H.P. (2002) ICL670A: preclinical profile. *Advances in experimental medicine and biology,* **509,** 185-203.

Piga, A., Galanello, R., Forni, G.L., Cappellini, M.D., Origa, R., Zappu, A., Donato, G., Bordone, E., Lavagetto, A., Zanaboni, L., Sechaud, R., Hewson, N., Ford, J.M., Opitz, H. & Alberti, D. (2006) Randomized phase II trial of deferasirox (Exjade, ICL670), a once-daily, orally-administered iron chelator, in comparison to deferoxamine in thalassemia patients with transfusional iron overload. *Haematologica,* **91,** 873-880.

Porter, J. & Hershko, C. (2012) The properties of Clinically useful Iron Chelators *Iron Phyisology and Pathophysiology in Humans , Editors Anderson HJ and McLaren GD. Humana Press (Book). ,* **Chapter 28,** 591-630.

Porter, J.B. (2006) Deferasirox: An effective once-daily orally active iron chelator. *Drugs of today,* **42,** 623-637.

Porter, J.B., Gyparaki, M., Burke, L.C., Huehns, E.R., Sarpong, P., Saez, V. & Hider, R.C. (1988) Iron mobilization from hepatocyte monolayer cultures by chelators: the importance of membrane permeability and the iron-binding constant. *Blood,* **72,** 1497-1503.

Porter, J.B., Morgan, J., Hoyes, K.P., Burke, L.C., Huehns, E.R. & Hider, R.C. (1990) Relative oral efficacy and acute toxicity of hydroxypyridin-4-one iron chelators in mice. *Blood,* **76,** 2389-2396.

Porter, J.B., Rafique, R., Srichairatanakool, S., Davis, B.A., Shah, F.T., Hair, T. & Evans, P. (2005) Recent insights into interactions of deferoxamine with cellular and plasma iron pools: Implications for clinical use. *Annals of the New York Academy of Sciences,* **1054,** 155-168.

Porter, J.B., Wood, J., Olivieri, N., Vichinsky, E.P., Taher, A., Neufeld, E., Giardina, P., Thompson, A., Moore, B., Evans, P., Kim, H.Y., Macklin, E.A. & Trachtenberg, F. (2013) Treatment of heart failure in adults with thalassemia major: response in patients randomised to deferoxamine with or without deferiprone. *Journal of cardiovascular magnetic resonance : official journal of the Society for Cardiovascular Magnetic Resonance,* **15,** 38.

Tallarida, R.J. (2006) An overview of drug combination analysis with isobolograms. *The Journal of pharmacology and experimental therapeutics,* **319,** 1-7.

Tanner, M.A., Galanello, R., Dessi, C., Smith, G.C., Westwood, M.A., Agus, A., Roughton, M., Assomull, R., Nair, S.V., Walker, J.M. & Pennell, D.J. (2007) A randomized, placebo-controlled, double-blind trial of the effect of combined therapy with deferoxamine and deferiprone on myocardial iron in thalassemia major using cardiovascular magnetic resonance. *Circulation,* **115,** 1876-1884.

Waldmeier, F., Bruin, G.J., Glaenzel, U., Hazell, K., Sechaud, R., Warrington, S. & Porter, J.B. (2010) Pharmacokinetics, metabolism, and disposition of deferasirox in beta-thalassemic patients with transfusion-dependent iron overload who are at pharmacokinetic steady state. *Drug metabolism and disposition: the biological fate of chemicals,* **38,** 808-816.

Yesim Aydinok, Kattamis, A., M Domenica Cappellini, El-Beshlawy, A., Origa, R., Elalfy, M., Kilinç, Y., Perrotta, S., Karakas, Z., Viprakasit, V., Habr, D., Antje Wegener, Shen, J. & Porter, J.B. (2013) Deferasirox–Deferoxamine Combination Therapy Reduces Cardiac Iron With Rapid Liver Iron Removal In Patients With Severe Transfusional Iron Overload (HYPERION). *Blood***,** 2257.

Table 1

Physicochemical properties of the chelators studied

Chelator	Molecular Weight	Chelator : iron (III) binding ratio	Stability Constant *log* β*n*	pM	Charge of free ligand	Charge of iron complex	Lipid Solubility of free ligand *(Kpart)*	Lipid Solubility of iron complex *(K part)*
DFO	561*	1 : 1	33 (1)	26.6	1+	1+	0.01	0.03
DFP	139	3 : 1	37.2	20.5	0	0	0.17	0.08
DFX	373	2 : 1	26.5	22.5	1-	3-	6.3	NK
CP40	169	3 : 1	36.7	19.9	0	0	0.08	0.001
CP46	182	3 : 1	36.5	20.1	1+	3+	0.008	0.0007

Figure 1

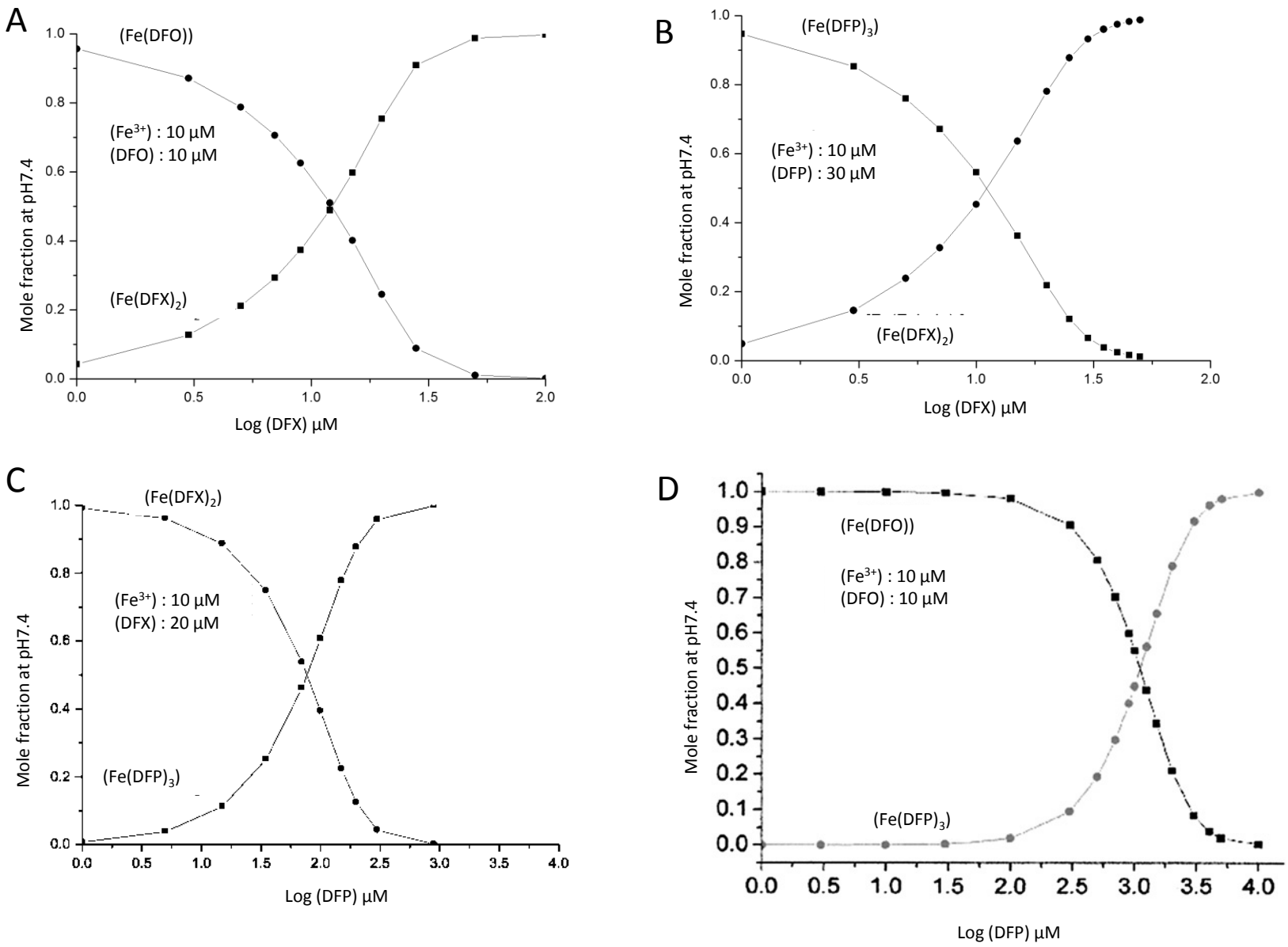
A
(Fe(DFO))
(Fe3+) : 10 µM
(DFO) : 10 µM
(Fe(DFX)2)
Mole fraction at pH7.4
Log (DFX) µM
B
(Fe(DFP)3)
(Fe3+) : 10 µM
(DFP) : 30 µM
(Fe(DFX)2)
Mole fraction at pH7.4
Log (DFX) µM
C
(Fe(DFX)2)
(Fe3+) : 10 µM
(DFX) : 20 µM
(Fe(DFP)3)
Mole fraction at pH7.4
Log (DFP) µM
D
(Fe(DFO))
(Fe3+) : 10 µM
(DFO) : 10 µM
(Fe(DFP)3)
Mole fraction at pH7.4
Log (DFP) µM

Figure 2

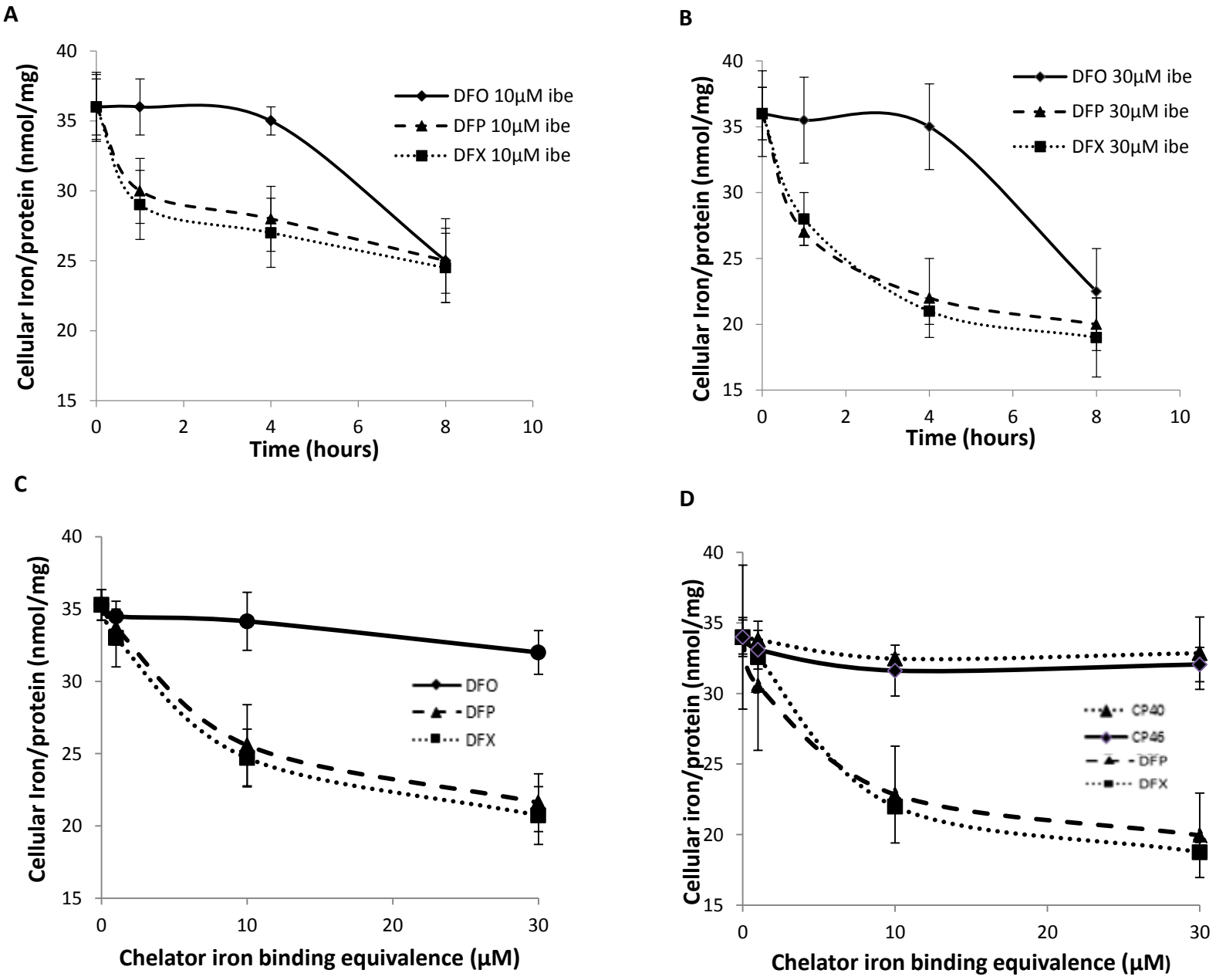
A
Cellular Iron/protein (nmol/mg)
Time (hours)
DFO 10μM ibe
DFP 10μM ibe
DFX 10μM ibe
B
Cellular Iron/protein (nmol/mg)
Time (hours)
DFO 30μM ibe
DFP 30μM ibe
DFX 30μM ibe
C
Cellular Iron/protein (nmol/mg)
Chelator iron binding equivalence (μM)
DFO
DFP
DFX
D
Cellular iron/protein (nmol/mg)
Chelator iron binding equivalence (μM)
CP40
CP46
DFP
DFX

Figure 3

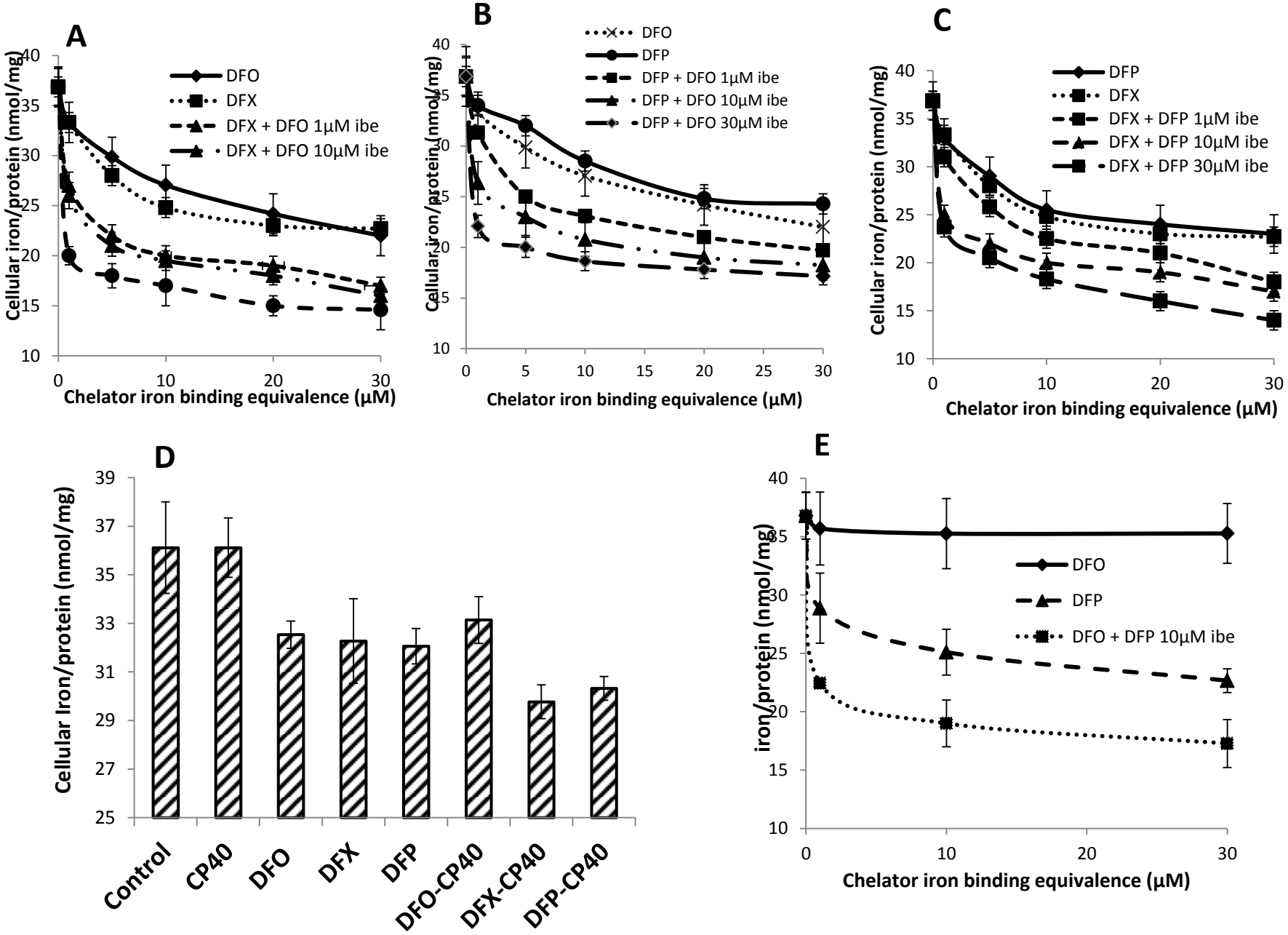
A
Cellular iron/protein (nmol/mg)
Chelator iron binding equivalence (μM)
DFO
DFX
DFX + DFO 1μM ibe
DFX + DFO 10μM ibe
B
Cellular iron/protein (nmol/mg)
Chelator iron binding equivalence (μM)
DFO
DFP
DFP + DFO 1μM ibe
DFP + DFO 10μM ibe
DFP + DFO 30μM ibe
C
Cellular iron/protein (nmol/mg)
Chelator iron binding equivalence (μM)
DFP
DFX
DFX + DFP 1μM ibe
DFX + DFP 10μM ibe
DFX + DFP 30μM ibe
D
Cellular Iron/protein (nmol/mg)
Control
CP40
DFO
DFX
DFP
DFO-CP40
DFX-CP40
DFP-CP40
E
iron/protein (nmol/mg)
Chelator iron binding equivalence (μM)
DFO
DFP
DFO + DFP 10μM ibe

Figure 4

A. Sample Isobologram

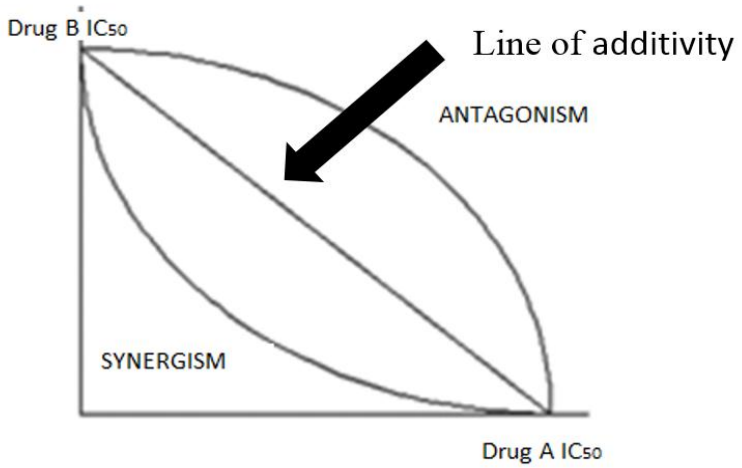

B. DFO- DFX Combination Isobologram

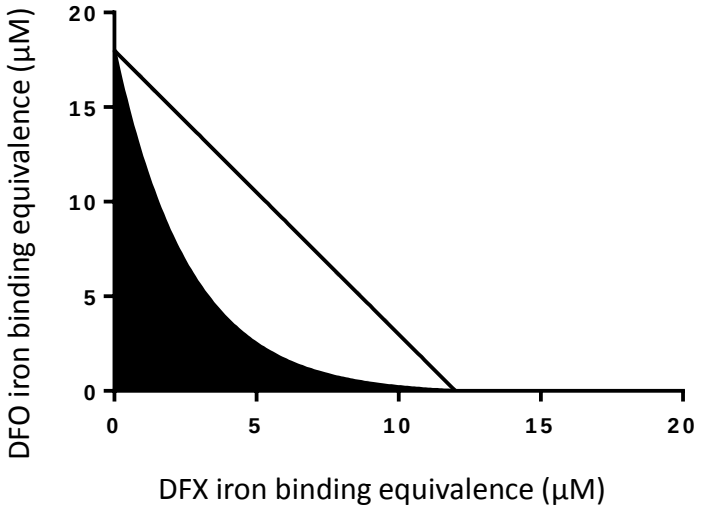

C. DFX- DFP Combination Isobologram

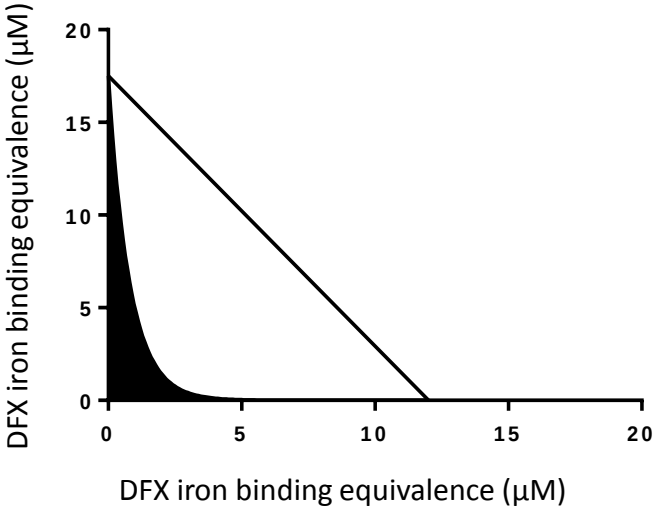

D.DFO- DFP Combination Isobologram

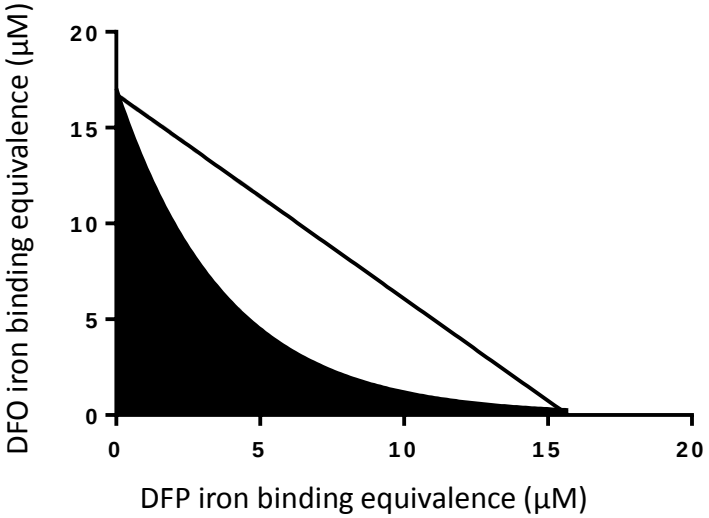

Table 2

Chelator Combination	Combination Index (CI)				Synergy Index 'α'
	ED_{20}	ED_{30}	ED_{50}	R (each combination fit)	
DFO + DFX	0.18	0.27	0.50	0.91	37
DFO + DFP	0.16	0.29	0.47	0.89	47.4
DFX + DFP	0.086	0.15	0.38	0.93	51.5

Table 3

Chelator Combination	Dose Reduction Index (DRI) of sink chelator	Shuttle Chelator Concentration (µM ibe) when in combination	Sink Chelator Concentration (µM ibe) when in combination
DFO + DFX	3.2 (DFO)	DFX 1.8µM ibe	DFO 5µM ibe
DFO + DFP	2.8 (DFO)	DFP 1.2µM ibe	DFO 5.7µM ibe
DFX + DFP	3.8 (DFX)	DFP 0.9µM ibe	DFX 3.4µM ibe